Available online at www.sciencedirect.com

SciVerse ScienceDirect

Ceramics International 39 (2013) 4499–4506

CERAMICS INTERNATIONAL

www.elsevier.com/locate/ceramint

Template synthesis and characterization of mesoporous γ-Al_2O_3 hollow nanorods using *Stevia rebaudiana* leaf aqueous extract

Mirla Rodríguez[a], Ángela B. Sifontes[a,*], Franklin J. Méndez[a], Yraida Díaz[a], Edgar Cañizales[b], Joaquín L. Brito[a,*]

[a]*Centro de Química, Instituto Venezolano de Investigaciones Científicas, Apartado 20632, Caracas 1020-A, Venezuela*
[b]*Área de Análisis Químico Inorgánico. PDVSA. INTEVEP. Los Teques 1070-A, Venezuela*

Received 17 October 2012; received in revised form 16 November 2012; accepted 18 November 2012
Available online 23 November 2012

Abstract

Mesoporous γ-Al_2O_3 hollow nanorods have been synthesized using aluminum isopropoxide as Al source and *Stevia rebaudiana* leaf extract (a complex mixture of eight sweet diterpene glycosides including stevioside, rebaudioside A, rebaudioside B, rebaudioside C, rebaudioside D, rebaudioside E, dulcoside and steviol bioside) as template to direct the formation of mesoporous alumina on the aqueous system. Several characterization techniques were used, including XRD, TGA, N_2 physical adsorption, FE-SEM, TEM, and FT-IR. By drying the mixture at 80 °C and then calcining it at 650 °C, a material with high surface area (357 m^2/g) and uniform pore sizes was obtained. The diameter and the length of the synthesized hollow nanorods ranged from 13 to 25 nm and from 40 to 50 nm respectively.

Keywords: γ-Al_2O_3; Hollow nanorods; *Stevia rebaudiana*

1. Introduction

Alumina has widespread applications in the field of advanced ceramics and it is mainly used as refractory materials, electrical insulators, in electronics, as catalysts, catalytic supports or adsorbents and for ceramic membranes. Particularly, γ-Al_2O_3 is widely used in catalysis or as adsorbent due to its high porosity and surface area [1].

Recently, the synthesis of nanostructured Al_2O_3 with 1-D morphology has drawn attention [2–15] due to their unique applications in nanodevices under extreme conditions such as high temperatures.

These nanostructures have been synthesized following a diversity of synthetic routs, some of which include the use of templates. Zhu et al. reported the synthesis of Al_2O_3 with a fiber morphology and large porosity using a nonionic surfactant [2,3]. Moreover, the synthesis of Al_2O_3 nanotubes and nanowires has been performed from anodic porous Al_2O_3 membranes [4–6], by thermal evaporation [7], electrochemically [8], using the sol–gel method [9], by coating and filling of carbon nanotubes [10], and by hydrothermal or solvothermal treatments [11]. In addition, Ma et al. [12] reported the synthesis of boehmite and γ-Al_2O_3 nanorods by a solvothermal route using $AlCl_3 \cdot 6H_2O$ in water-aniline binary mixtures, as well as the synthesis of γ-Al_2O_3 nanorods using $AlCl_3 \cdot 6H_2O$, NaOH and sodium dodecilbenzene sulfonate in water–dimethylbenzene mixtures [13]. Li et al. [14] reported the synthesis of γ-Al_2O_3 nanorods by an arc-discharge method from Fe and Al powders. Tang et al. [15] showed the preparation of boehmite nanoneedles, nanorods and nanotubes by the hydrothermal method from $Al(NO_3)_3 \cdot 9H_2O$. Hou et al. [16] applied a hydrothermal method for the synthesis of boehmite nanotubes and nanorods using aluminum tricloride and sodium amide.

Hollow mesoporous structures have emerged as rapidly growing research themes and have been widely applied in

*Corresponding authors. Tel.: +58 212 5041342; fax: +58 212 5041340.
E-mail addresses: angelasifontes@gmail.com (Á.B. Sifontes), joabrito@ivic.gob.ve (J.L. Brito).

0272-8842/$ - see front matter © 2012 Elsevier Ltd and Techna Group S.r.l. All rights reserved.
http://dx.doi.org/10.1016/j.ceramint.2012.11.044

many important fields, such as catalysis, controlled release of drugs, confined synthesis, opto-electronics, and energy storage, owing to their properties of low density, high surface areas, and interstitial hollow spaces [17]. Several synthetic strategies for hollow mesoporous structures have been developed, including well known hard/soft-templating methods, Kirkendall or Ostwald ripening effects, and selective etching [18]. Templating is the common method to fabricate hollow materials. However, these templates are mostly used to prepare hollow spherical micro-sized particles [19].

Nowadays, much research is oriented to the development of eco-friendly synthesis methods, using less toxic and low cost chemicals as reactants. In recent years, *S. rebaudiana* leaf extract, which contains a complex mixture of eight sweet diterpene glycosides including stevioside, rebaudioside A, rebaudioside B, rebaudioside C, rebaudioside D, rebaudioside E, dulcoside and steviol bioside [20] has been successfully used for the synthesis of gold and silver nanoparticles [21–23]. To our best knowledge, the synthesis of nanosized porous metal oxides using *S. rebaudiana* has not been reported.

The aim of the study carried out in this research work was to synthesize mesoporous γ-Al_2O_3 hollow nanorods an aqueous medium by using *S. rebaudiana* leaf extract as template.

2. Experimental

2.1. Preparation of the S. rebaudiana leaf extract.

Portions of 1.2 g of leaves of *S. rebaudiana* were extracted with 50 mL of hot water (65 °C) for 3 h, as described by Nishiyama et al. [24]. The crude extract was filtered through a Whatman qualitative filter paper no. 1.

2.2. Synthesis

Synthesis of mesoporous γ-Al_2O_3 was carried out from aqueous solutions employing aluminum isopropoxide (Sigma-Aldrich) as precursor and *S. rebaudiana* leaf extract as template. In a typical preparation, 4.2 g of aluminum isopropoxide was dissolved in 54 mL of distilled water.

The formation of alumina using metal alkoxide as precursor usually takes place according to the following reaction scheme [25]:

$$Al(OR)_3 + 2H_2O \rightarrow AlOOH + 3ROH \quad (1)$$

$$2AlOOH \overset{600\ ^\circ C}{\rightarrow} Al_2O_3 + H_2O \quad (2)$$

The resultant solution was magnetically stirred at room temperature for 2 h, and then, the extract was added dropwise. The pH value was adjusted to 5 using a diluted acid nitric aqueous solutions. The obtained solution was evaporated and dried at 80 °C for 48 h and the resulting solid was calcined to remove the template. This was carried out in a tubular furnace under air atmosphere, with a heating rate of 5 °C/min up to 650 °C and kept at the maximum temperature for 6 h.

2.3. Characterization

Characterization was carried out by X-ray diffraction, using a Siemens D-5005 diffractometer and CuKα radiation in the 2θ range between 5° and 70°, operating at 40 kV and 20 mA. Thermogravimetric analysis (TGA) was performed from room temperature up to 750 °C in a Du Pont 990 thermogravimetric analyzer under an air flow (100 mL/min) at a heating rate of 10 °C/min. Fourier transform infrared (FT-IR) spectra were recorded for samples prepared before and after calcination employing a Perkin Elmer 100 spectrometer in the range of 2000–500 cm^{-1}. The textural properties of the calcined oxide were characterized by N_2 adsorption porosimetry (Micromeritics, ASAP 2010). The sample was degassed at 300 °C under vacuum. Nitrogen adsorption isotherm was measured at liquid N_2 temperature (77 K), and N_2 pressures ranging from 10^{-6} to $1.0P/P_0$. The surface area was calculated following the Brunauer–Emmett–Teller (BET) method [24] and the pore size distribution was obtained according to the Barret–Joyner–Halenda (BJH) method

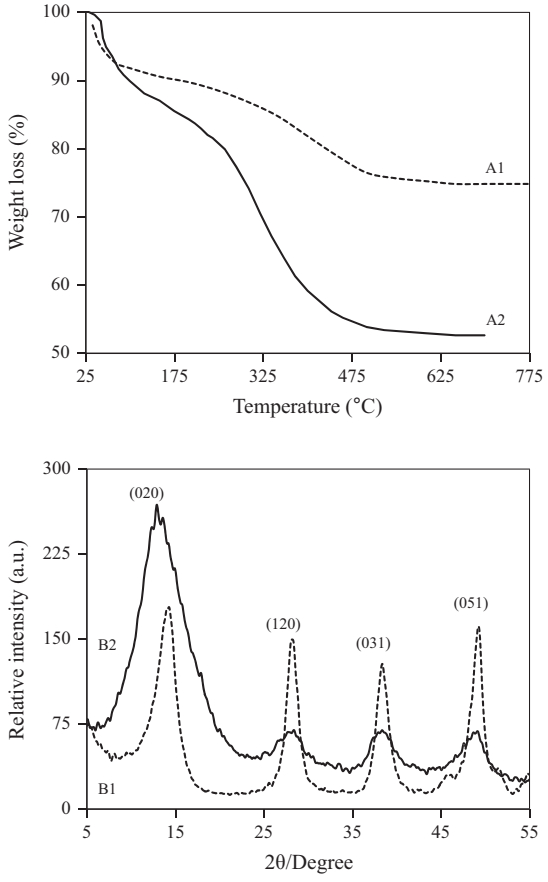

Fig. 1. TGA curves of the pure boehmite and as-synthesized sample dried at 80 °C (A1 and A2, respectively). XRD patterns of pure boehmite and as-synthesized sample dried at 80 °C (B1 and B2, respectively).

[26].The morphologies were observed by field emission scanning electron microscopy (FE-SEM), using a Quanta 250 FEG scanning electron microscope (accelerating voltage of 30 kV). The evaluation by transmission electron microscopy (TEM) was performed in a Hitachi 7100 microscope. All samples were prepared by suspending the powders in an ethanol-based liquid and placing the suspension onto a carbon/collodion-coated 200 mesh copper grid.

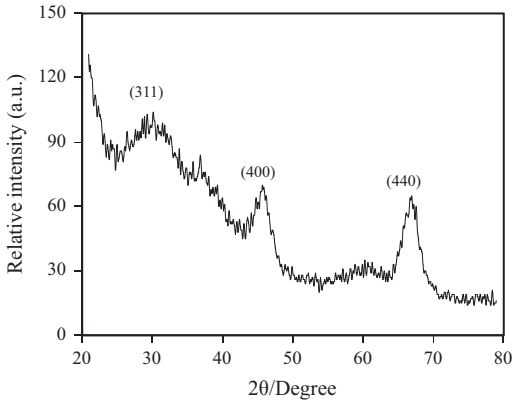

Fig. 2. XRD patterns of synthesized γ-Al_2O_3.

3. Results and discussion

The study of the thermal decomposition of the as-synthesized samples could help understand the interaction between the diterpene glycosides and the inorganic precursor.

According to Eqs. (1) and (2), the presence of boehmite was expected as an intermediate product, prior to the calcination step. Fig. 1(A1, A2) present, respectively, the TG curves of pure boehmite and as-synthesized sample

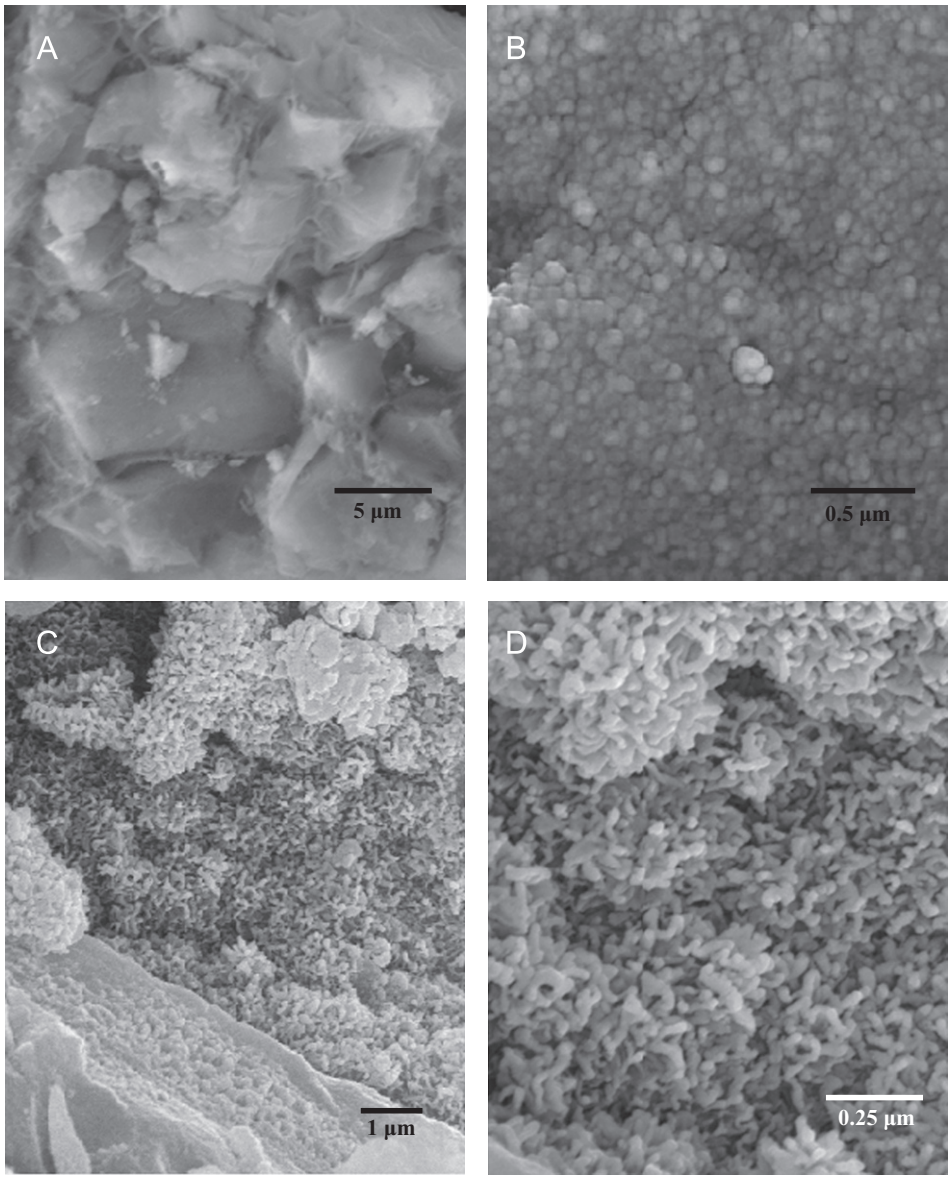

Fig. 3. FE-SEM image of sample γ-Al_2O_3 after calcination at 650 °C: (A) 8000 ×, (B) 60,000 ×, (C) 14,000 ×, and (D) 60,000 ×.

dried at 80 °C. With the aim of comparing, pure boehmite was synthesized in the absence of the extract. The dehydroxylation of boehmite to γ-Al_2O_3 is known to occur at temperatures higher than 300 °C, and it involves a theoretical weight loss of 15% [27]. This was observed in the temperature range 100–500 °C in the pure boehmite sample (Fig. 1-A1). Nevertheless, the observed weight loss at the former temperature interval for the as-synthesized sample was much higher than the theoretical value (37.1%). This could be attributed to the decomposition of the diterpene glycosides–boehmite complex also generated in the synthesis medium during the dehydroxylation of boehmite. The TGA of the as-synthesized sample (Fig. 1-A2) showed several weight losses between 30 and 550 °C, while no changes were evident above 550 °C. This TG curve could be divided into three regions of weight loss. The first one (zone I) between 25 and 150 °C corresponds to the desorption of physisorbed water [27,28]. Weight loss in the 150–300 °C region (zone II), was attributed to removal of most of the template [27,28]. Zone III, (300–600 °C) could be assigned to the loss of water associated with the phase change to form γ-alumina, and decomposition and elimination altogether of the remaining organic compounds that helped form the pore structure. The ''plateau'' observed above 550 °C in the TG curve indicated that a stable phase had been formed.

X-ray diffraction patterns corresponding to the pure boehmite (JCPDS Card 21-1307) and as-synthesized sample are presented in Fig. 1-B1 and B2. The location of some broad and weak peaks observed in the case of the as-synthesized sample dried at 80 °C confirmed the presence of the boehmite phase [29–31]. The (020) reflection is especially important [29–31], since it is a characteristic of compounds with laminar structure perpendicular to the [010] direction. Furthemore, the reflection (020) presents a greater *d*-spacing (6.88 Å) as compared to the pure boehmite (6.27 Å) [29–31]. This can be attributed to the presence of intercalated water molecules between boehmite octahedra double layers [32,33]. Bokhimi et al. [32], and Baker and pearson [33], proposed that this particularly occurs in boehmite samples of very small crystal size. Another possibility regards the hydroxyl groups bonded to aluminum atoms on a crystal surface. The oxygen atoms of these hydroxyl surfaces have a free orbital that gives rise to hydrogen bonds when crystals grow perpendicularly to the surface. If crystal growth is hindered, these oxygen atoms can react easily with the aqueous environment. In an acidic medium, which is the present case, the free orbital will react with a proton, forming an aquo ligand bonded to an aluminum atom [32,33].

In addition, it was observed that the intensity of the (020) peak in the boehmite standard used in this research (Fig. 1-B2) was greater than the other peaks. Therefore, the (020) planes are the prefered growth direction of AlOOH.

The crystalline properties of the synthesized γ-Al_2O_3 are shown by the XRD pattern in Fig. 2. The XRD trace presents two main peaks placed at *d*-spacings of 0.197, and 0.140 nm, corresponding respectively to the (400) and (440) reflections of γ-Al_2O_3 [27]. The general shape of the DRX trace agrees with the poor crystallinity of this type of transitional phase.

Fig. 3 shows FE-SEM micrographs of the calcined sample. These results confirm that the alumina particles formed at 650 °C have laminated structure (Fig. 3A). On the other hand, it seems that these structures consist of aggregates of nanoparticles with a tubular morphology and particle size around 50 nm (Fig. 3 A–D).

The laminar structure of the synthesized alumina is intrinsically consistent with the plate like morphology, which is a characteristic of the boehmite phase [27,29–32]. This was attributed to the topotactic transformation of boehmite that

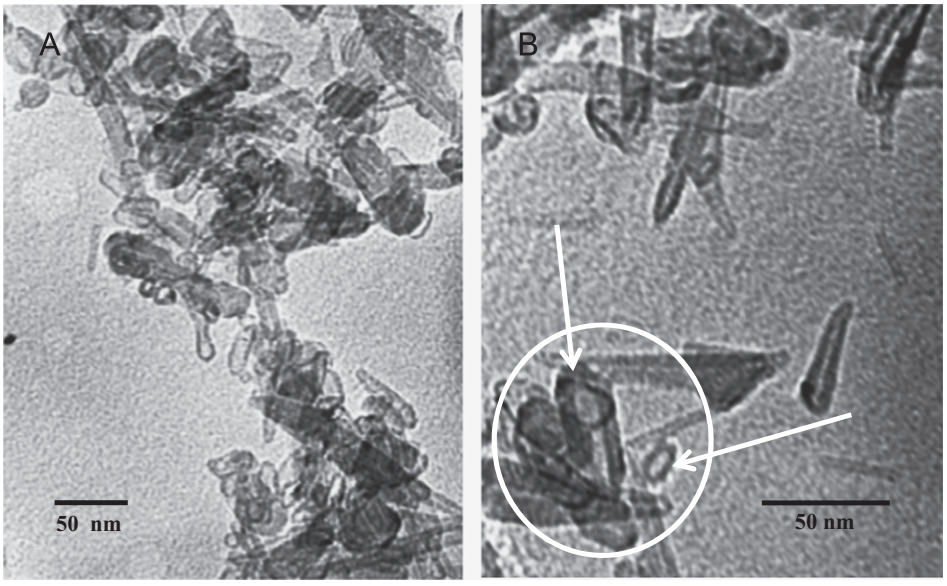

Fig. 4. TEM image of sample γ-Al_2O_3 after calcination at 650 °C: (A) 105,000 × and (B) 167,000 × . The circle shows the open end of a hollow nanorod.

takes place during calcination at temperatures around 600–800 °C [34]. These results are consistent with the characterization made by XRD and TGA, which suggested the presence of boehmite as an intermediate stage.

Fig. 4 shows the TEM image of the γ-Al_2O_3 nanoparticles. It is clearly observed that synthesized γ-Al_2O_3 consists of a large quantity of hollow nanorods with lengths around 50 nm and ranging diameters from 13 to 25 nm. The observed morphology in the synthesized materials could be the result of a complex system of intermolecular interactions between the diterpene glycosides molecules and the alumina precursor, with the subsequent formation of a hybrid organic–inorganic composite. It has been reported that classic hydrogen bonds may cause mainly the formation of discrete (0D) supramolecular structures, molecular dimers, and in some cases the formation of 1D chain structures [35,36]. In this sense, observations of the structural formula of steviol bioside have indicated that the hydrophilic part of the molecule has dimensions that are comparable with the hydrophobic tetracyclic fragment. These compounds may therefore interact preferentially and form lamellar structures with alternating layers composed of predominant hydrophilic and hydrophobic molecular fragments [35].

On the other hand, under synthesis conditions, the diterpene glycoside molecules could be solvated since the water and isopropyl alcohol are present in the reaction medium [35]. Also, glycoside residue and tetracyclic molecular frame would be situated one above the other forming an intramolecular cavity [35]. Subsequently, the interaction of the boehmite inorganic precursor with the former structure and the heating treatment at 650 °C would allow the production of alumina with the morphology of hollow rods.

Fig. 5 shows the N_2 adsorption–desorption isotherms and pore size distribution of synthesized γ-Al_2O_3. This material presented a type IV isotherm (as defined by IUPAC) [22] which is a characteristic of mesoporous materials. The appearance of a type H2 hysteresis loop indicates the presence of "ink-bottle" type pores in the mesoporous Al_2O_3 [22]. The physisorption measurements revealed a high BET surface area (357 m^2/g) and a pore size distribution centered at 4.8 nm. In addition, it was observed that the pore sizes of the mesoporous γ-Al_2O_3 seems irrespective of the rods diameter of the γ-Al_2O_3 nanorods. Therefore, the mesoporous structure was probably originated mainly from the voids between grains after calcinations. This agrees with the morphology observed by SEM (Fig. 3). TEM micrographs indicated that most hollow nanorods possess closed ends and only a fraction presents one or both open ends (Fig. 4B). This could justify the shoulders observed in the pore-size distribution curve at 11 and 14 nm diameters (Fig. 5B).

Fig. 6(A) shows the FT-IR spectrum of the as-synthesized sample with *S. rebaudiana* extract. The most characteristic signals correspond to the absorption bands around 1659 cm^{-1} and 1419–1445 cm^{-1}, which can be

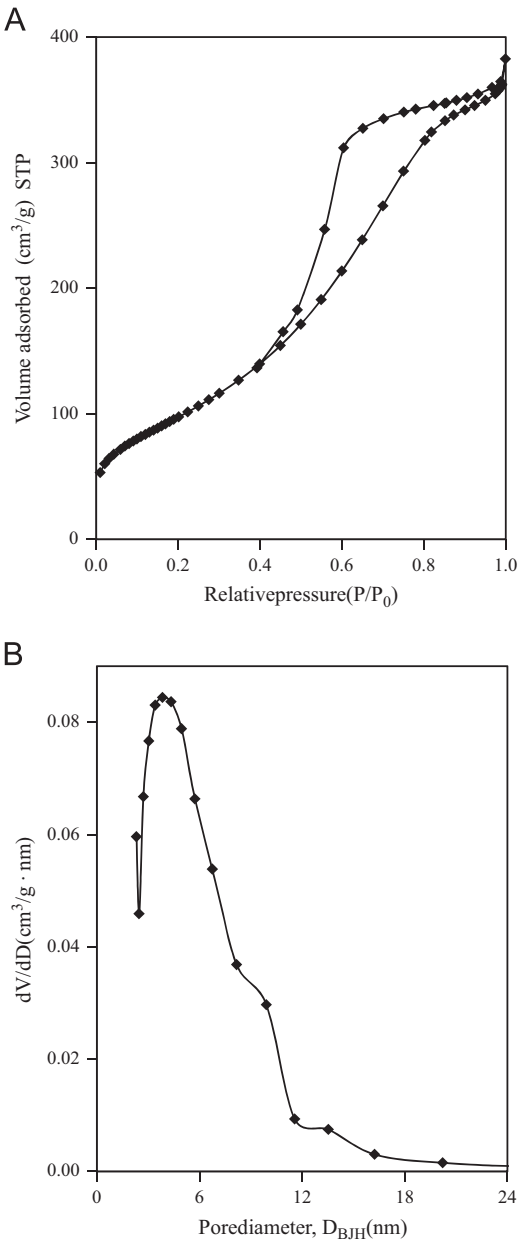

Fig. 5. (A) Nitrogen adsorption–desorption isotherm and (B) pore size distribution calculated from the desorption branch of the mesoporous γ-Al_2O_3.

assigned to the stretching vibrational [37] modes of carboxylate groups (COO-) generated in the synthesis medium. These carboxylate groups are bound to the aluminum atoms present on the surface of the boehmite. Furthermore, the strong signal at 1380 cm^{-1}, could reveal the presence of free carboxylate groups that are not coordinated to the aluminum atoms [37]. This can be attributed to the acid hydrolysis of the stevioside [38], a diterpenoid glycoside (Fig. 7B and C) which can generate diterpenic molecules like steviol and isosteviol as products [38]. Both compounds, could interact with the metal monohidroxide (boehmite) through these carboxylate groups, and coordinate similarly to the formation of aluminum ionic complexes in solution.

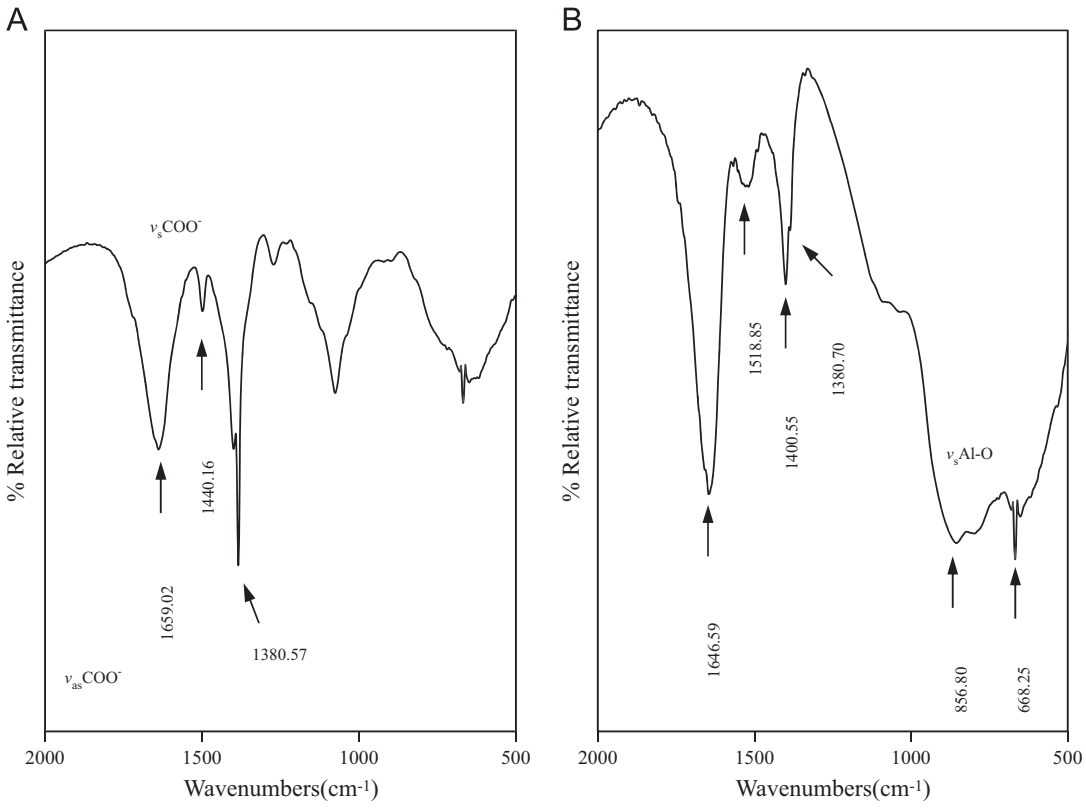

Fig. 6. FT-IR spectra of the as-synthesized sample (A) and calcined sample (B).

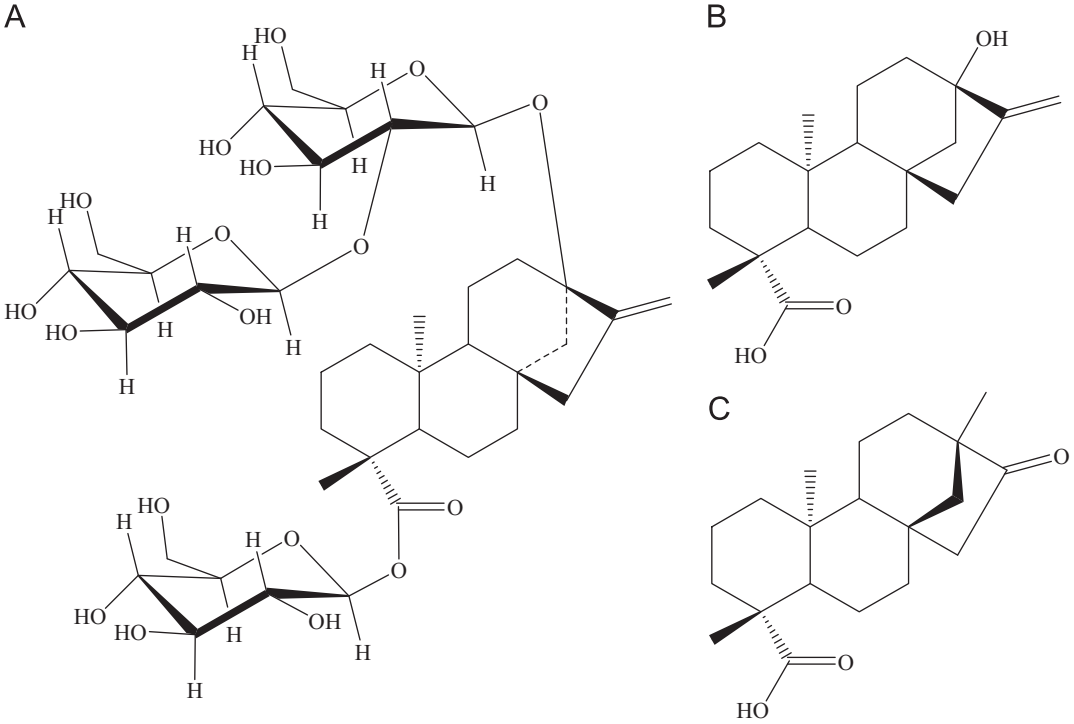

Fig. 7. Structure of stevioside (A) steviol (B) and isosteviol (C).

FT-IR absorption bands were observed in the sample calcined at 650 °C (Fig. 6B) and were associated with structurally different aluminum superficial sites. On the surface of alumina particles, two coordinatively different types of aluminum ions can be found [39–42]: tetrahedral (Td) and octahedral (Oh), with coordination numbers of

four and six, respectively. The FT-IR spectra show absorption bands in the range of 500–750 cm^{-1} due to the stretching vibrations of AlO bonds of the octahedrally coordinated Al. On the other hand, bands due to vibrations of AlO bond in AlO_4 units are present around 750–900 cm^{-1} [39–42].

4. Conclusions

Mesoporous γ-Al_2O_3 hollow nanorods were synthesized through a facile, low-cost and non-surfactant-templating synthesis route. *S. rebaudiana* leaf extract was used to direct the formation of the porous structure. The alumina powders obtained exhibited an high surface area (357 m^2/g) and uniform pore sizes. The particle size of the alumina synthesized in this research ranged in diameter from 13 to 25 nm with lengths between 40 and 50 nm.

Acknowledgments

The authors would like to acknowledge the fine technical assistance of Freddy Sanchez (TEM).

References

[1] Z. Zhu, H. Sun, H. Liu, D. Yang, PEG-directed hydrothermal synthesis of alumina nanorods with mesoporous structure via AACH nanorod precursors, Journal of Materials Science 45 (2010) 46–50.
[2] H.Y. Zhu, J.D. Riches, J.C. Barry, γ-Alumina nanofibers prepared from aluminum hydrate with polyethylene oxide surfactant, Chemistry of Materials 14 (2002) 2086–2093.
[3] H.Y. Zhu, X.P. Gao, D.Y. Song, S.P. Ringer, Z. Gao, Y.X. Xi, W. Martens, J.D. Riches, R.L. Frost, Growth of boehmite nanofiber by assembling nanoparticles with surfactant micelles, Journal of Physical Chemistry B 108 (2004) 4245–4247.
[4] Y.F. Mei, X.L. Wu, X.F. Shao, G.S. Huang, G.G. Siu, Formation mechanism of alumina nanotube array, Physics Letters A 309 (2003) 109–113.
[5] Y.F. Mei, X.L. Wu, X.F. Shao, G.G. Siu, X.M. Bao, Formation of an array of isolated alumina nanotubes, Europhysics Letters 62 (2003) 595–599.
[6] L. Zhang, B. Cheng, W.S. Shi, E.T. Samulski, *In-situ* electrochemical synthesis of 1-dimensional alumina nanostructures, Journal of Materials Chemistry 15 (2005) 4889–4893.
[7] Q. Zhao, X. Xu, H. Zhang, Y. Chen, J. Xu, D. Yu, Catalyst-free growth of single-crystalline alumina nanowire arrays, Applied Physics A: Materials Science and Processing 79 (2004) 1721–1724.
[8] W. Lee, K. Schwirn, M. Steinhart, E. Pippel, R. Scholz, U. Gösele, Structural engineering of nanoporous anodic aluminium oxide by pulse anodization of aluminium, Nature Nanotechnology 3 (2008) 234–239.
[9] S.C. Kuiry, E. Megen, S.D. Patil, S.A. Deshpande, S. Seal, Solution-based chemical synthesis of boehmite nanofibers and alumina nanorods, Journal of Physical Chemistry B 109 (2005) 3868–3872.
[10] J.S. Lee, B. Min, K. Cho, S. Kim, J. Park, Y.T. Lee, N.S. Kim, M.S. Lee, S.O. Park, J.T. Moon, Al_2O_3 nanotubes and nanorods fabricated by coating and filling of carbon nanotubes with atomic-layer deposition, Journal of Crystal Growth 254 (2003) 443–448.
[11] H.C. Lee, H.J. Kim, S.H. Chung, K.H. Lee, J.C. Lee, Synthesis of unidirectional alumina nanostructures without added organic solvents, Journal of the American Chemical Society 125 (2003) 2882–2883.
[12] M.-G. Ma, Y.-J. Zhu, G.-F. Cheng, Y.-H. Huang, Solvothermal synthesis of boehmite and γ-Al_2O_3 nanorods, Journal of Materials Science and Technology 24 (2008) 637–640.
[13] M.-G. Ma, Y.-J. Zhu, X.-L. Xu, A new route to synthesis of γ-Al_2O_3 nanorods, Materials Letters 61 (2007) 1812–1815.
[14] W.F. Li, X.I. Ma, W.S. Zhang, W. Zhang, Y. Li, Z.D. Zhang, Synthesis and characterization of γ-Al_2O_3 nanorods, Physica Status Solidi A 203 (2006) 295–299.
[15] B. Tang, J.C. Ge, L.H. Zhuo, G.L. Wang, J.Y. Niu, Z.Q. Zhi, Y.B. Dong, A facile and controllable synthesis of γ-Al_2O_3 nanostructures without a surfactant, European Journal of Inorganic Chemistry 21 (2005) 4366–4369.
[16] H.W. Hou, Y. Xie, Q. Yang, Q.X. Guo, C.R. Tan, Preparation and characterization of γ-AlOOH nanotubes and nanorods, Nanotechnology 16 (2005) 741–745.
[17] X. Fang, Z. Liu, M.-F. Hsieh, M. Chen, P. Liu, Ch. Chen, N. Zheng, Hollow mesoporous aluminosilica spheres with perpendicular pore channels as catalytic nanoreactors, ASC Nano 6 (2012) 4434–4444.
[18] M.-H. Park, Y.H. Cho, K. Kim, J. Kim, M. Liu, J. Cho, Germanium nanotubes prepared by using the Kirkendall effect as anodes for high-rate lithium batteries, Angewandte Chemie—International Edition 50 (2011) 9647–9650.
[19] G. Fu, A. He, Y. Jin, Q. Cheng, J. Song, Fabrication of hollow silica nanorods using nanocrystalline cellulose as templates, Bioresources 7 (2012) 2319–2329.
[20] A. Esmat Abou-Arab, A. Azza Abou-Arab, M. Ferial Abu-Salem, Physicochemical assessment of natural sweeteners steviosides produced from stevia rebaudiana, African Journal of Food Science 4 (2010) 269–281.
[21] A.N. Mishra, S. Bhadauria, M.S. Gaur, R. Pasricha, B.S. Kushwa, Synthesis of gold nanoparticles leaves of zero-calorie sweetener herb (*Stevia rebaudiana*) and their nanoscopic characterization by spectroscopy and microscopy, International Journal of Green Nanotechnology: Physics and Chemistry 1 (2010) 118–124.
[22] R. Varshney, S. Bhadauria, M.S. Gaur, Biogenic synthesis of silver nanocubes and nanorods using sundried *Stevia rebaudiana*, Advanced Materials Letters 1 (2010) 232–237.
[23] M. Yilmaz, H. Turkdemir, M. Akif Kilic, E. Bayram, A. Cicek, A. Mete, B. Ulug, Biosynthesis of silver particles using leaves of *Stevia rebaudiana*, Materials Chemistry and Physics 130 (2011) 1195–1202.
[24] P. Nishiyama, M. Alvarez, L.G. Vieira, Quantitative analysis of stevioside in the leaves of *Stevia rebaudiana* by near infrared reflectance spectroscopy, Journal of the Science of Food and Agriculture 59 (1992) 277–281.
[25] C. Márquez, V. González, I. Díaz, M. Grande, T. Blasco, J. Pérez, Sol–gel synthesis of mesostructured aluminas from chemically modified aluminum sec-butoxide using non-ionic surfactant templating, Microporous Mesoporous Materials 80 (2005) 173–182.
[26] S.J. Gregg, K.S.W. Sing, in: Adsorption, Surface Area and Porosity, second ed., Academic Press, London, 1982.
[27] Q. Liu, A. Wang, X. Wang, T. Zhang, Mesoporous γ-alumina synthesized by hydro-carboxylic acid as structure-directing agent, Microporous Mesoporous Materials 92 (2006) 10–21.
[28] H.C. Lee, H.J. Kim, C.H. Rhee, K.H. Lee, J.S. Lee, S.H. Chung, Synthesis of nanostructured γ-alumina with a cationic surfactant and controlled amounts of water, Microporous Mesoporous Materials 79 (2005) 61–68.
[29] D. Mishra, S. Anand, R.K. Panda, R.P. Das, Hydrothermal preparation and characterization of boehmites, Materials Letters 42 (2000) 38–45.
[30] K. Okada, T. Nagashima, Y. Kameshima, A. Yasumori, T. Tsukada, Relationship between formation conditions, properties, and crystallite size of boehmite, Journal of Colloid and Interface Science 253 (2002) 308–314.
[31] Y. Liu, D. Ma, X. Han, X. Bao, W. Frandsen, D. Wang, D. Su, Hydrothermal synthesis of microscale boehmite and gamma nanoleaves alumina, Materials Letters 62 (2008) 1297–1301.

[32] X. Bokhimi, J.A. Toledo-Antonio, M.L. Guzman Castillo, F. Hernandez-Beltran, Relationship between crystallite size and bond lengths in boehmite, Journal of Solid State Chemistry 159 (2001) 32–40.
[33] B.R. Baker, R.M. Pearson, Water content of pseudoboehmite: a new model for its structure, Journal of Catalysis 33 (1974) 265–278.
[34] X. Krokidis, P. Raybaud, A. Gobichon, B. Rebours, P. Euzen, H. Toulhoat, Theoretical study of the dehydration process of boehmite to γ-alumina, Journal of Physical Chemistry B 105 (2001) 5121–5130.
[35] A.T. Gubaidullin, D.V. Beskrovnyj, I.A. Litvinov, Crystal structure model based on the analysis of hydrophilic–hydrophobic ratio in molecules. Isosteviol derivatives, Chinese Journal of Structural Chemistry 46 (2005) 195–201.
[36] A.T. Gubaidullin, V.A. Mamedov, I.A. Litvinov, H. Ye, S. Tsuboi, Synthesis and comparative analysis of molecular and supramolecular structures of 4,8-disubstituted 1,5-dichloro-2,6-dioxotricyclo[5.1.0.0 3,5]octanes, Monatshefte fur Chemie 134 (2003) 1229–1240.
[37] R.M. Silverstein, F.X. Webster, David Kiemle, in: Spectrometric Identification of Organic Compounds, seventh ed., John Wiley Inc., New York, 2005.
[38] H.M.S. Milagre, L.R. Martins, J.A. Takahashi, Novel agents for enzymatic and fungal hydrolysis of stevioside, Brazilian Journal of Microbiology 40 (2009) 367–372.
[39] P. Padmaja, G.M. Anilkumar, P. Mukindan, G. Aruldhas, K.G.K. Warrier, Characterisation of stoichiometric sol–gel mullite by fourier transform infrared spectroscopy, International Journal of Inorganic Materials 3 (2001) 693–698.
[40] Ph. Colomban, Structure of oxide gels and glasses by infrared and Raman scattering., Journal of Materials Science 24 (1989) 3002–3010.
[41] P. Mc Millan, B. Piriou, The structures and vibrational spectra of crystals and glasses in the sílica–alumina system, Journal of Non-Crystalline Solids 53 (1982) 279–298.
[42] K. Okada, N. Otsuka, S. Somiya, Review of mullite synthesis routes in Japan, American Ceramic Society Bulletin 70 (1991) 1633–1640.